ISSN 0036-0236, Russian Journal of Inorganic Chemistry, 2010, Vol. 55, No. 7, pp. 1042–1051. © Pleiades Publishing, Ltd., 2010.
Original Russian Text © I. Bulhac, P.N. Bouroş, O.A. Bologa, V. Lozan, O. Ciobanică, J. Lipkowski, T.F. Mitina, Yu.A. Simonov, 2010, published in Zhurnal Neorganicheskoi Khimii, 2010, Vol. 55, No. 7, pp. 1111–1121.

Specific Features of the Structures of Iron(II) α-Benzyl Dioxymate Solvates with Pyridine

I. Bulhac[a], **P. N. Bouroş** [b], **O. A. Bologa**[a], **V. Lozan**[a], **O. Ciobanică**[a], **J. Lipkowski**[c], **T. F. Mitina**[a], **and Yu. A. Simonov**[b]
[a] *Institute of Chemistry, Academy of Sciences of Moldova, Chisinau, Moldova*
[b] *Institute of Applied Physics, Academy of Sciences of Moldova, Chisinau, Moldova*
[c] *Institute of Physical Chemistry, Polish Academy of Sciences, Warsaw, Poland*

Received December 18, 2008

Abstract—Coordination compounds $[Fe(DfgH)_2Py_2]$ (**I**) and $[Fe(DfgH)_2Py_2] \cdot A$, where DfgH is the α-benzyldioxime monoanion and A = Py (**II**), DMF (**III**), and methyl ethyl ketone (**IV**), have been synthesized and studied by X-ray diffraction analysis. Diamagnetism and the gamma-resonance (GR) spectral parameters confirm that iron exists in the oxidation state +2 in the low-spin state. The octahedral *trans* configuration of the iron polyhedra is a common feature of all complexes. The equatorial plane of the octahedron contains two intramolecular hydrogen bonds O–H···O between two organic anions $DfgH^-$ affording a pseudomacrocycle. The axial coordinate of the octahedron is occupied by the pyridine molecules, which are almost perpendicular to the equatorial plane N_4(oxime) in complexes **I–IV**. The structure of the compounds is a framework with allowance for weak interactions C–H···O and C–H···C. The manner of inclusion of solvents into the crystal and their functioning in structure formation of compounds **II–IV** are discussed.

DOI: 10.1134/S0036023610070090

L.A. Chugaev pioneered in studying the complex formation of α-dioximes (α-$DioxH_2$) with transition metals, including iron [1]. The coordination of the central atom in the α-dioximate complexes is mainly defined by the nature of the complexing metal: square for nickel(II) [2–4], platinum(II) [5–7], palladium(II) [6, 8], and cobalt(II) [9]; square-pyramidal (dimeric) for copper(II) [10, 11]; octahedral for cobalt(III) [12–17], iron(II) [18–21], and iron(III) [22]. A new method for the synthesis of iron(II) dioximates with biologically active ligands, including potentially polydentate pyridine derivatives, has been described [23, 24]. Coordination compounds with transition metals synthesized under the conditions providing the deprotonation of the α-$DioxH_2$ molecules are characterized by the general structural architecture: two single-charge organic ligands (α-$DioxH^-$) lie nearly in one plane, coordinating the metal through the nitrogen atoms to form the central core MN_4, which results in the formation of two five-membered metallocycles. This structure is stabilized by two intramolecular hydrogen bonds of the O–H···O type between the organic ligands, thus creating two pseudo-six-membered metallocycles. As a whole, they form one pseudomacrocycle. Similar architecture was found in the square transition metal complexes [2–9]. This architecture also forms the base for tetragonal pyramids in copper(II) dimers [10, 11] and is observed in the equatorial part of octahedral complexes [12–22]. In an acidic medium, the deprotonation of α-$DioxH_2$ is hindered and, hence, no intramolecular hydrogen bonds of the O–H···O type and, correspondingly, no pseudomacrocycles are formed in such complexes. Under these conditions, nickel(II), cobalt(II), copper(II), and iron(II) form with α-$DioxH_2$ monomeric *cis*-dioximines [25, 26] and tris(dioximines) [27–29]. In the presence of KI, Cu(II) is reduced to Cu(I) with the formation of the 1D polymer $[Cu(NioxH_2)I]_\infty$ ($NioxH_2$ is 1,2-cyclohexanedionedioxime) in which the iodide anions act as bridges and the polyhedron of the metal atom is a tetrahedron [30]. Although the structure of metal *cis*- and tris(dioximines) remains octahedral, it differs substantially from that of traditional dioximates: there are no intramolecular hydrogen bonds O–H···O between α-$DioxH_2$; two and three molecules in the case of *cis*-dioximines and tris(dioximines), respectively, lie in two and three mutually perpendicular planes.

The iron(II) atom in $[Fe(DfgH)_2Py_2]$ (**I**) and $[Fe(DfgH)_2Py_2] \cdot DMF$ (**III**) ($DfgH_2$ is α-benzyldioxime) is easily oxidized by such oxidants as Cl_2 [31], Br_2 [32], and I_2 [33] to form $[Fe(DfgH)_2Py_2]X$ ($X = Cl^- \cdot Cl_2$, Br_3^-, I_5^-). This process is reversible [33, 34]. However, it should be mentioned that, in all cases, the reduction of $[Fe(DfgH)_2Py_2]X$ affords complex **I** as hexagonal cherry-colored plates resembling crystals of compound **III** in shape and color and substantially different from Chugaev's compound of the same formula $[Fe(DfgH)_2Py_2]$ (**Ia**) (dark brown, almost black elongated prisms). In an excess of pyridine and methyl

Table 1. Crystallographic data and experimental characteristics for structures **I**–**IV**

	I	II	III	IV
FW	692.55	771.65	838.74	836.75
Crystal system	Orthorhombic	Monoclinic	Monoclinic	Monoclinic
Space group	*Pbca*	$P2_1/c$	*C*2/*c*	*C*2/*m*
Unit cell parameter				
a, Å	11.4207(8)	9.024(1)	13.8600(4)	10.185(2)
b, Å	16.5160(10)	11.482(2)	10.0030(4)	13.825(1)
c, Å	17.657(2)	18.719(3)	30.168(1)	15.559(2)
β, deg	90	102.69(2)	92.037(2)	107.523(11)
V, Å^3	3330.5(5)	1892.2(8)	4179.9(3)	2089.1(5)
Z	4	2	4	2
ρ_{calcd}, g/cm^3	1.381	1.354	1.333	1.330
μ, mm^{-1}	0.504	0.452	0.419	0.418
F(000)	1440	804	1760	880
Crystal sizes, mm	0.20 × 0.20 × 0.10	0.30 × 0,20 × 0.10	0.25 × 0.20 × 0.10	0.22 × 0.22 × 0.07
θ range, deg	2.31–26.07	2.23–25.50	2.83–23.23	2.59–26.21
Reflection index ranges	$-14 \le h \le 14$	$-10 \le h \le 10$	$-15 \le h \le 15$	$-12 \le h \le 9$
	$-20 \le k \le 20$	$-13 \le k \le 13$	$-11 \le k \le 11$	$-17 \le k \le 15$
	$-21 \le l \le 21$	$-22 \le l \le 22$	$-33 \le l \le 33$	$-19 \le l \le 19$
Number of measured/independent reflections	25176/3284 [$R_{int} = 0.0577$]	14168/3386 [$R_{int} = 0.0455$]	17913/2978 [$R_{int} = 0.1078$]	4456/2153 [$R_{int} = 0.0324$]
Number of reflections with $I > 2\sigma(I)$	2008	2107	2357	1754
Number of refined parameters	223	250	268	152
GOOF	0.796	1.002	1.150	0.944
R ($I > 2\sigma(I)$)	$R1 = 0.0337$ $wR2 = 0.0742$	$R1 = 0.0411$ $wR2 = 0.0890$	$R1 = 0.0792$ $wR2 = 0.1542$	$R1 = 0.0486$ $wR2 = 0.1216$
R (over the whole set)	$R1 = 0.0604$ $wR2 = 0.0784$	$R1 = 0.0660$ $wR2 = 0.0922$	$R1 = 0.1017$ $wR2 = 0.1634$	$R1 = 0.0622$ $wR2 = 0.1281$
$\Delta\rho_{max}$, $\Delta\rho_{min}$, eÅ^{-3}	0.390, –0.320	0.355, –0.231	0.655, –0.333	1.080, –0.355

ethyl ketone (MEK), $[Fe(DfgH)_2Py_2] \cdot Py$ (**II**) and $[Fe(DfgH)_2Py_2] \cdot CH_3C(O)C_2H_5$ (**IV**), respectively, are formed. The crystals of pyridine products **I**–**IV** differ in color and shape from one another and from Chugaev's complex **Ia**, which appears, most likely, due to the effect of solvent molecules on the formation of the crystal structure. The coordination compounds containing the same iron(II) complex (**I**) and its analogues with different solvents, namely, Py (**II**), DMF (**III**), and MEK (**IV**), were synthesized to elucidate the role of the solvent in the architecture of the crystals. The crystal structures of compounds **I**–**IV** were determined by X-ray diffraction analysis.

EXPERIMENTAL

Synthesis of compound I. Iron(II) chloride tetrahydrate (0.033 g, 0.17 mmol) was dissolved in methanol (25 mL) (solution 1), α-benzyldioxime (0.08 g, 0.33 mmol) was dissolved in pyridine (4 mL) (solution 2), and sodium acetate trihydrate (0.027 g, 0.20 mmol) was dissolved in methanol (20 mL) (solution 3). Solutions 2 and 3 were alternately added in small portions to solution 1 with continuous stirring. A vessel with the cherry-colored solution was left closed. Single crystals as black octahedra were formed after two months. Compound **I** was obtained in a yield of 0.075 g. The yield based in $FeCl_2 \cdot 4H_2O$ was 65%.

For $C_{38}H_{32}FeN_6O_4$ anal. calcd. (%): C, 65.84; H, 4.65; N, 12.13; Fe, 8.06.

Found (%): C, 65.60; H, 5.02; N, 12.20; Fe, 8.02.

Synthesis of compound II. Iron(II) chloride tetrachloride (0.4 g, 2.012 mmol) was dissolved in methanol (10 mL). A warm solution of α-benzyldioxime (0.96 g, 4.0 mmol) in pyridine (10 mL) was added to the obtained solution. Crystals as elongated dark brown prisms were formed after ~15 min. The final

Table 2. Selected interatomic distances (*d*) and bond angles (ω) in structures **I–IV**

Bond	**I**	**II**	**III**	**IV**
	d, Å			
Fe(1)–N(1)	1.906(2)	1.904(2)	1.891(4)	1.896(2)
Fe(1)–N(2)	1.897(2)	1.896(2)	1.892(4)	–
Fe(1)–N(3)	2.027(2)	2.018(2)	1.999(5)	2.007(3)
N(1)–O(1)	1.353(2)	1.364(2)	1.366(5)	1.358(2)
N(1)–C(1)	1.317(3)	1.310(3)	1.317(7)	1.308(3)
N(2)–O(2)	1.370(2)	1.363(2)	1.373(5)	–
N(2)–C(2)	1.313(3)	1.304(3)	1.308(7)	–
C(1)–C(11)	1.479(3)	1.484(3)	1.483(8)	1.487(3)
C(1)–C(2)	1.486(3)	1.474(3)	1.475(7)	1.475(4)
C(2)–C(21)	1.481(3)	1.491(3)	1.482(8)	–
N(3)–C(31)	1.348(3)	1.327(4)	1.348(7)	1.345(3)
C(31)–C(32)	1.375(3)	1.376(5)	1.376(9)	1.382(4)
C(32)–C(33)	1.370(4)	1.340(5)	1.369(9)	1.382(3)
C(33)–C(34)	1.378(4)	1.356(5)	1.382(9)	1.382(9)
C(34)–C(35)	1.373(3)	1.374(4)	1.383(9)	–
N(3)–C(35)	1.345(3)	1.338(4)	1.344(7)	–

II		**III**		**IV**	
Bond	*d*, Å	Bond	*d*, Å	Bond	*d*, Å
N(4)–C(3)	1.321(5)	O(3)–C(5)	1.25(1)	O(3)–C(5)	1.26(1)
C(3)–C(4)	1.331(5)	N(4)–C(5)	1.32(1)	C(3)–C(4)	1.38(2)
N(4)–C(4)#2	1.325(5)	N(4)–C(4)	1.41(1)	C(4)–C(5)	1.33(2)
C(4)–C(5)#2	1.325(5)	N(4)–C(3)	1.46(1)	C(5)–C(6)	1.34(1)
C(4)–N(4)#2	1.325(5)				

Angle	**I**	**II**	**III**	**IV**
	ω, deg			
N(1)Fe(1)N(2)	80.74(7)	80.87(8)	80.7(2)	98.80(11)
N(1)Fe(1)N(2)#1	99.26(7)	99.13(8)	99.3(2)	81.20(11)
N(1)Fe(1)N(3)	87.16(7)	89.62(8)	88.7(2)	88.57(8)
N(1)Fe(1)N(3)#1	92.84(7)	90.38(8)	91.3(2)	91.43(8)
N(2)Fe(1)N(3)	88.17(7)	89.86(9)	89.1(2)	–
N(2)Fe(1)N(3)#1	91.83(7)	90.14(9)	90.9(2)	–
O(1)N(1)Fe(1)	122.2(1)	122.4(2)	122.9(3)	122.9(1)
C(1)N(1)Fe(1)	117.1(1)	117.2(2)	117.9(4)	117.0(2)
O(2)N(2)Fe(1)	122.4(1)	122.6(1)	122.3(3)	–
C(2)N(2)Fe(1)	117.9(1)	117.1(2)	117.8(3)	–
C(31)N(3)Fe(1)	121.0(2)	123.8(2)	122.3(4)	121.5(2)
C(35)N(3)Fe(1)	121.9(2)	122.2(2)	121.3(4)	–
O(1)N(1)C(1)	119.8(2)	119.7(2)	119.1(4)	119.9(2)
O(2)N(2)C(2)	119.7(2)	120.1(2)	119.8(4)	–
N(1)C(1)C(2)	111.9(2)	111.5(2)	111.3(5)	112.3(1)
N(1)C(1)C(11)	124.4(2)	124.8(2)	123.1(5)	122.9(2)
C(2)C(1)C(11)	123.4(2)	123.1(2)	125.5(5)	124.5(1)

Table 2. (Contd.)

Angle	I	II	III	IV
	ω, deg			
C(1)C(11)C(12)	122.0(2)	121.9(3)	122.8(5)	121.9(2)
C(1)C(11)C(16)	119.4(2)	118.9(3)	117.6(5)	118.9(2)
N(2)C(2)C(1)	111.7(2)	112.8(2)	112.2(5)	–
N(2)C(2)C(21)	124.3(2)	124.0(2)	122.0(5)	–
C(1)C(2)C(21)	123.9(2)	123.0(2)	125.6(5)	–
C(2)C(21)C(22)	120.2(2)	120.0(3)	122.0(5)	–
C(2)C(21)C(26)	121.3(2)	121.4(3)	119.0(5)	–
C(31)N(3)C(35)	116.8(2)	114.0(3)	116.3(5)	116.8(3)
N(3)C(31)C(32)	122.8(2)	124.5(3)	123.3(6)	123.3(2)
C(31)C(32)C(33)	120.0(3)	120.6(3)	119.4(6)	119.1(3)
C(32)C(33)C(34)	117.6(2)	116.6(3)	118.8(6)	118.3(4)
C(33)C(34)C(35)	120.1(3)	120.3(3)	118.5(6)	–
N(3)C(35)C(34)	122.7(2)	124.0(3)	123.7(6)	–

IV: N2 = N1#2, N2# = N1#3, C2 = C1#3, C35 = C31#3, C34 = C32#3

II		III		IV	
Angle	ω, deg	Angle	ω, deg	Angle	ω, deg
C(3)N(4)C(4)#2	18.8(4)	C(5)N(4)C(4)	123.2(8)	C(3)C(4)C(5)	145(2)
N(4)C(3)C(4)	120.3(4)	C(5)N(4)C(3)	120.7(8)	C(5)#4C(5)O(3)	130.5(7)
C(5)#2C(4)C(3)	120.9(4)	C(4)N(4)C(3)	116.0(8)	O(3)C(5)C(6)	119(1)
N(4)#2C(4)C(3)	120.9(4)	O(3)C(5)N(4)	123.0(8)	O(3)C(5)C(4)	112(2)
				C(6)C(5)C(4)	127(1)

* Symmetry codes:

I: #1 –*x*, –*y* + 2, –*z* + 1;

II: #1 –*x* + 1, –*y*, –z; #2 –*x* + 2, –*y* + 1, –*z* + 2;

III: #1 –*x* + 1/2, –*y* + 1/2, –*z*;

IV: #1 –*x*, –*y*, –*z*; #2 –*x*, *y*, –*z*; #3 x, –*y*, *z*; #4 *x*, –*y* + 1, *z*.

Table 3. Intramolecular hydrogen bond geometry in structures **I**–**IV**

D–H···A	Distance, Å			Angle DHA, deg	Coordinates of atoms A
	D–H	H···A	D···A		
I					
O(1)–H···O(2)	0.83	1.71	2.517(2)	163	–*x*, –*y* + 2, –*z* + 1
II					
O(1)–H···O(2)	0.82	1.73	2.521(2)	163	–*x* + 1, –*y*, –*z*
III					
O(1)–H···O(2)	0.82	1.72	2.516(5)	162	–*x* + 1/2, –*y* + 1/2, –*z*
IV					
O(1)–H···O(2)	0.84	1.71	2.517(3)	162	–*x*, –*y*, –*z*

product was obtained in a yield of 1.46 g. The yield based on $FeCl_2 \cdot 4H_2O$ was 94%.

For $C_{43}H_{37}FeN_7O_4$ anal. calcd. (%): C, 66.91; H, 4.83; N, 12.71; Fe, 7.24.

Found (%): C, 67.13; H, 5.05; N, 12.99; Fe, 7.30.

Synthesis of compound III. Iron(II) chloride tetrahydrate (1.0 g, 5.03 mmol) was dissolved in methanol (25 mL) (solution 1). α-Benzyldioxime (2.4 g,

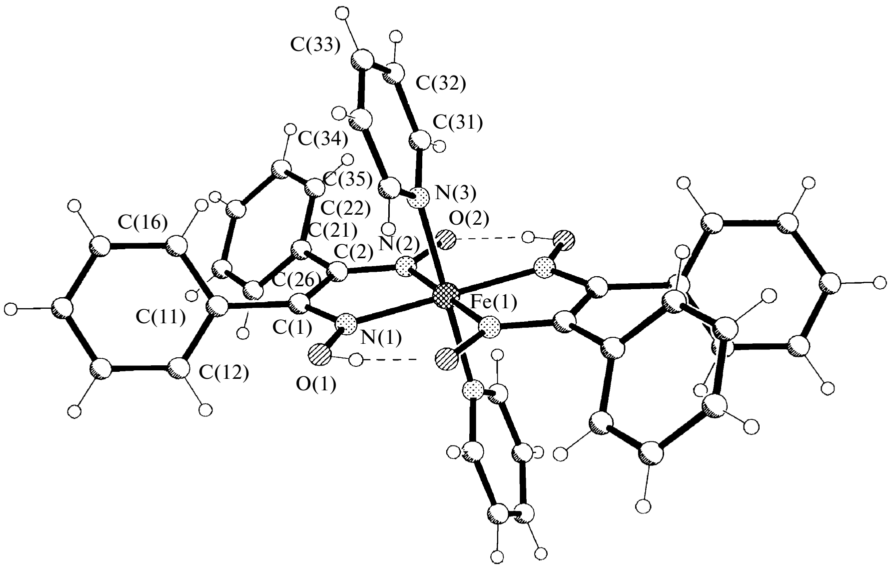

Fig. 1. Structure of the complex [Fe(DfgH)$_2$(Py)$_2$] (**I**).

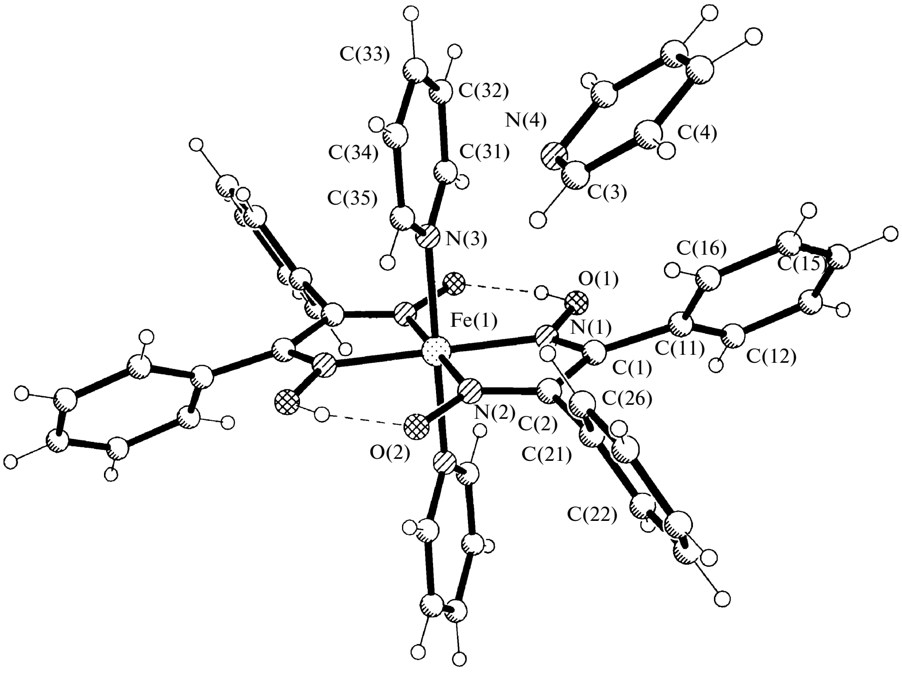

Fig. 2. Structure of the complex [Fe(DfgH)$_2$(Py)$_2$] · Py (**II**).

10.0 mmol) and pyridine (1 mL) were dissolved in DMF (25 mL) (solution 2). Solution 2 was added to solution 1 with continuous stirring. Upon pouring together these solutions, a finely crystalline product was formed as hexagonal red-cherry plates, which was separated from the mother liquor, washed with a DMF–methanol (1 : 1) mixture and then with a minor amount of methanol and diethyl ether, and dried in air. The final product was obtained in a yield of 3.20 g. The yield based on $FeCl_2 \cdot 4H_2O$ was 83%.

An absorption band at 1670 cm^{-1} assigned to ν(C=O) of DMF appears in the IR spectrum of compound **III**.

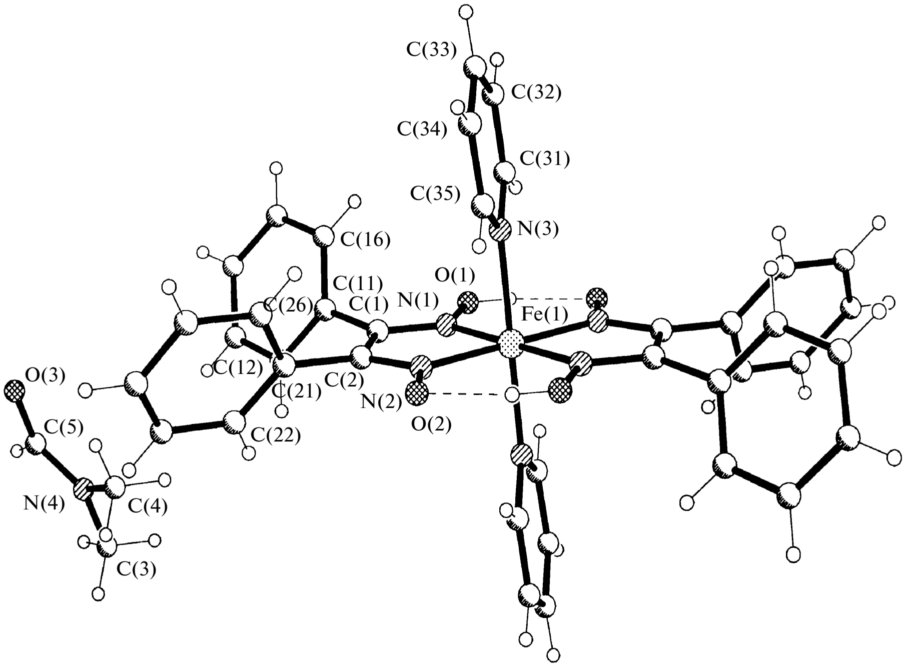

Fig. 3. Structure of the complex $[Fe(DfgH)_2(Py)_2] \cdot DMF$ (**III**).

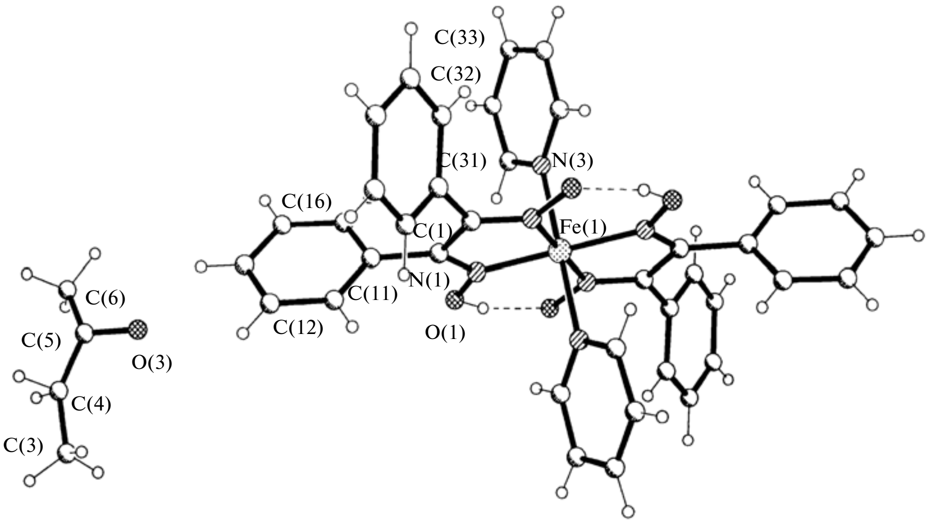

Fig. 4. Structure of the complex $[Fe(DfgH)_2(Py)_2] \cdot MEK$ (**IV**).

The single crystals suitable for X-ray diffraction were isolated from the mother liquor after its gradual evaporation in air.

For $C_{41}H_{39}FeN_7O_5$ anal. calcd. (%): C, 64.32; H, 5.13; N, 12.81; Fe, 7.29.

Found (%): C, 65.13; H, 5.15; N, 12.99; Fe, 7.30.

Synthesis of compound IV. Iron(III) bis(α-benzyldioximato)di(pyridine) polyiodide (2.0 g, 1.50 mmol) obtained by the oxidation of compound **I** with molecular iodine [33] was dissolved in MEK (80 mL). The solution was filtered off, and a 25% solution of ammonia (1 mL) was added with continuous stirring. Dark red crystals as large elongated hexagonal plates were formed after 20–30 min. The final product was obtained in a yield of 0.8 g. The yield based on $[Fe(DfgH)_2Py_2][I_5]$ was 70%.

For $C_{42}H_{40}FeN_6O_5$ anal. calcd. (%): C, 65.97; H, 5.27; N, 10.99; Fe, 7.30.

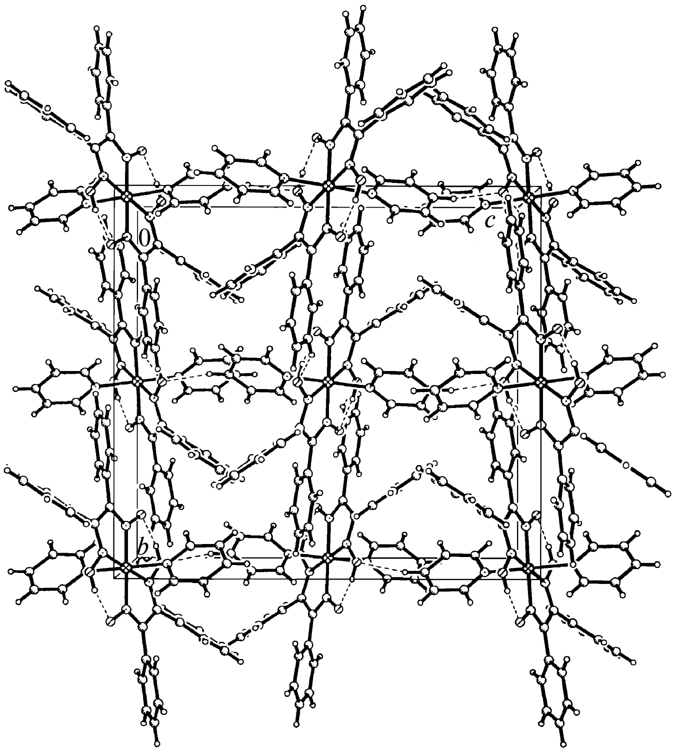

Fig. 5. Fragment of crystal structure **I**.

Found (%): C, 65.92; H, 5.01; N, 11.31; Fe, 7.27.

Compounds **I**–**IV** are diagmagnetic. The parameters of the GR spectra at 300 K are as follows: IS = 0.52–0.56 mm/s, QS = 1.92–1.94 mm/s; at 80 K, IS = 0.54–0.56 mm/s, QS = 1.93–1.96 mm/s (the accuracy of IS (relative to sodium pentacyanonitrosylferrate) and QS determination is ±0.04 mm/s [17]). These data confirm that iron exists in the low-spin state in the oxidation state +2.

GR spectra of the compounds were recorded on a constant acceleration spectrometer operating in the time mode. The ^{57}Co isotope in the chromium matrix at room temperature served as the source. Fine powders of the substances were used as absorbers, whose thickness was 5–10 mg/cm^2 by the natural isotopic composition.

X-ray diffraction analysis. The unit cell parameters and the reflection intensity sets for crystals of compounds **I**, **II**, and **IV** were obtained on a STOE IPDS-2T diffractometer (MoK_α radiation, graphite monochromator) at 213, 293, and 173 K, respectively. The experimental data were processed using the STOE X-AREA program [35]. For complex **III**, the experimental data were obtained at 200 K on a Nonius Kappa CCD diffractometer (MoK_α radiation, graphite monochromator, ω-2θ scan mode) [36]. The unit cell parameters were refined over the whole array of experimental data. The intensities were integrated and reduced to a common scale using the DENZO [37] and SKALEPACK [37] programs. Absorption corrections were applied by the XEMP program [38]. The structures of compounds **I**–**IV** were solved by direct methods and refined by least squares in the anisotropic full-matrix variant for non-hydrogen atoms (SHELX-97) [39]. Hydrogen atoms were revealed objectively and refined in the rigid body model.

The crystallographic data and experimental characteristics for structures **I**–**IV** are listed in Table 1. Selected interatomic distances and bond angles are given in Table 2. The hydrogen bonding geometry is presented in Table 3. The positional and thermal parameters for the structures of compounds **I**–**IV** were deposited with the Cambridge Crystallographic Data Centre (CCDC 706634–CCDC 706637).

RESULTS AND DISCUSSION

Compounds **I**–**IV** can be represented as complexes of general formula $[Fe(DfgH)_2(Py)_2] \cdot n$Solv, where $n = 0$ for **I**, $n = 1$ for **II**–**IV**; Solv is Py for **II**, DMF for **III**, and MEK for **IV**. The molecular structures of compounds **I**–**IV** and the atomic numbering scheme are shown in Figs. 1–4. The intrinsic symmetry of the complexes is C_i in **I**–**III** and C_{2h} in **IV**. The iron atoms have the *trans*-octahedral coordination mode similar to that found in the transition metal complexes of general formula $[M(DioxH)_2A_2]$, where A are neutral

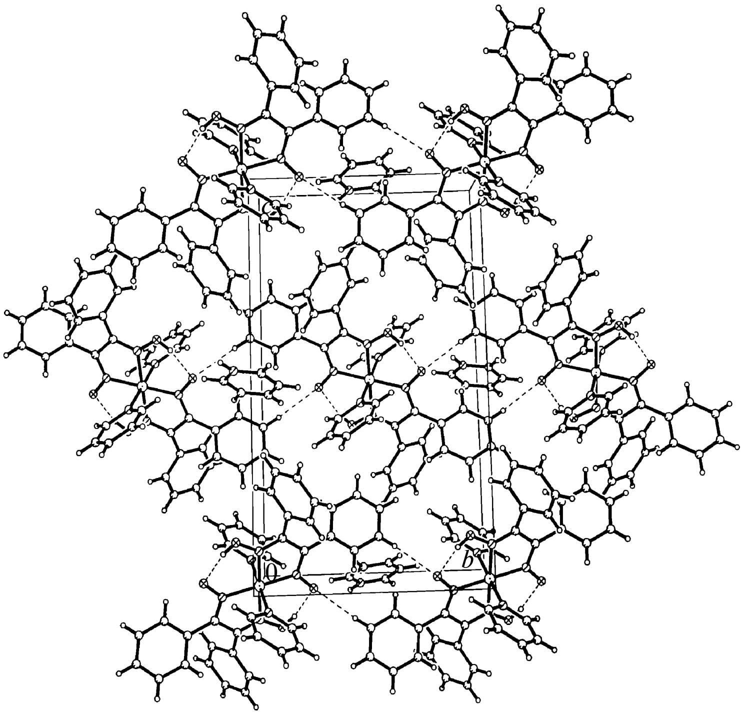

Fig. 6. Fragment of crystal structure **II**.

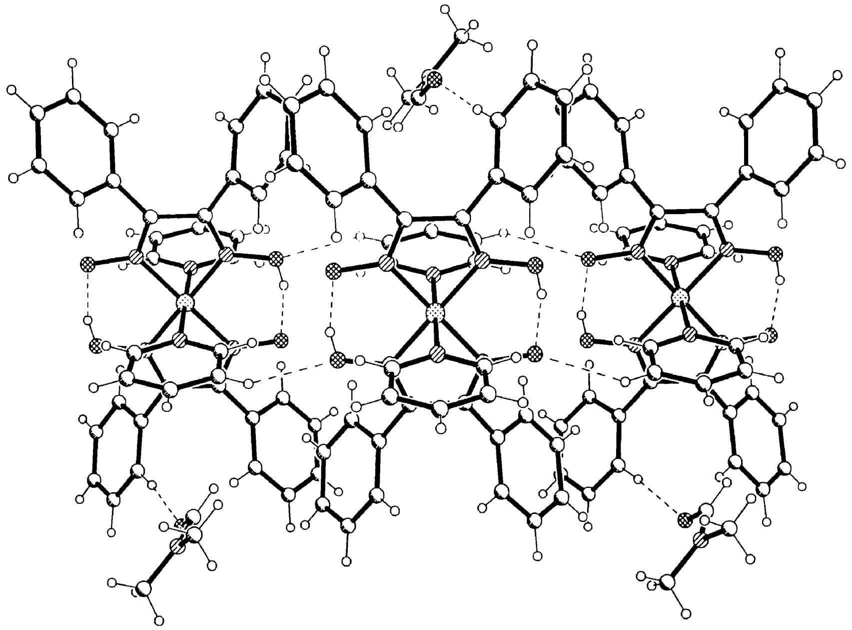

Fig. 7. Fragment of crystal structure **III**.

ligands (pyridine, aniline, thiourea, their derivatives, and others) [40]. The coordination polyhedron of the Fe(II) ion in structures **I**–**IV** is formed by six nitrogen atoms, four of which belong to two bidentate monodeprotonated $DfgH^-$ ligands, and two nitrogen atoms belong to two coordinated Py molecules.

In compounds **I**–**IV**, the Fe(1)–N(dioxime) interatomic distances are equal, on the average, to

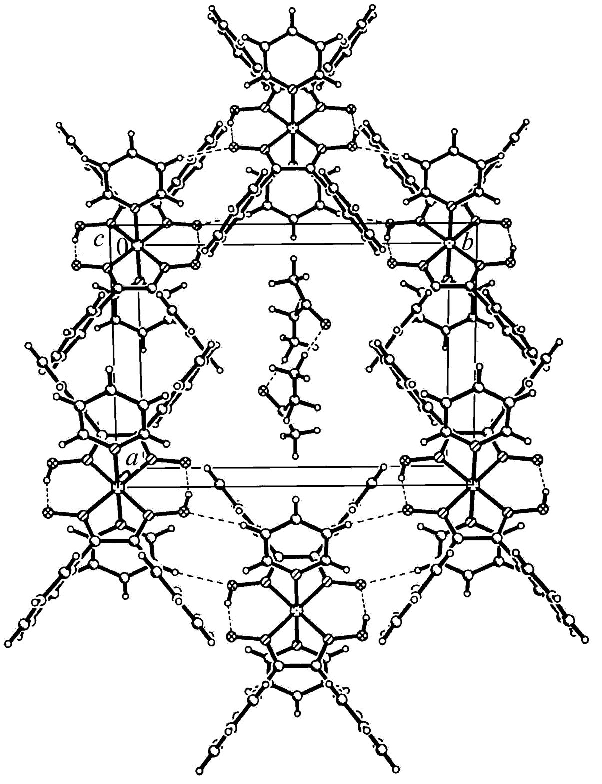

Fig. 8. Fragment of crystal structure **IV**.

1.902(2), 1.900(2), 1.896(2), and 1.891(4) Å, respectively. The Fe(1)–N(Py) bond lengths are 2.027(2), 2.018(2), 2.007(3), and 1.999(5) Å, respectively (Table 2). In each structure, the coordination octahedron of the iron atom is slightly elongated in the direction of the pyridine fragment. Possibly, the shortening of the Fe–N(dioxime) bond compared to Fe(1)–N(Py) is defined by both the chelating effect and the formation of the pseudomacrocyclic structure. The interatomic distances in compounds **I**–**IV** are close to those found in Fe(II) complexes with monodeprotonated α-benzyldioximes and coordinated apical molecules of pyridine derivatives [41]. The shortening of the Fe–N(dioxime) bonds is comparable with that in Fe(III) α-dioximates [22], which is defined by the bond redistribution in the pseudomacrocyclic system of the equatorial fragments conjugated with the aromatic rings. Each equatorial plane of complexes **I**–**IV** contains two α-benzyldioxime residues coordinated according to the N,N type, resulting in the formation of two chelate rings. This mutual arrangement of the $DfgH^-$ residues is fixed by the O–H···O intramolecular hydrogen bonds (Table 3). This leads to the fragments in which the five-membered metallocycles alternate with the six-membered pseudocycles formed through intramolecular hydrogen bonds. In coordinated α-dioximes, the average interatomic distances N–O, C=N, C–C, and C–C(Ph) are, respectively, 1.361(2), 1.315(3), 1.486(3), and 1.480(3) Å in **I**; 1.363(2), 1.307(3), 1.474(3), and 1.487(3) Å in **II**; 1.370(5), 1.313(7), 1.475(7), and 1.483(8) Å in **III**; 1.358(2), 1.308(3), 1.475(4), and 1.487(3) Å in **IV**. They are close to those found in the Fe(II) complexes with monodeprotonated α-benzyldioxime and pyridine derivatives: 1.357(3), 1.308(4), 1.466(4), and 1.482(4) Å in $[Fe(DfgH)_2(3\text{-}CONH_2\text{-}Py)_2]$ and 1.356(2), 1.313(3), 1.476(3), and 1.481(3) Å in $[Fe(DfgH)_2(4\text{-}COOC_2H_5\text{-}Py)_2]$ [41].

Two pyridine molecules are in the apical positions of the polyhedra of the central metal atom in structures **I**–**IV**. The dihedral angles between the planes of the aromatic ring of the latter and the equatorial N_4 atoms of the corresponding coordination polyhedra are 99.3°, 90.7°, 94.9°, and 95.9°. The deviations of the dihedral angle from 90° can be due to intermolecular interactions. The same factor defines the turn of the plane of the Py ligand about the Fe–N(Py) axis. Similar arrangement of the α-dioximates and neutral nitrogen-containing ligands was found in the iron(II) complexes with imidazole [19], nicotinamide and its derivative [41], and pyrazine [42]. The interatomic distances and bond angles in the coordinated Py molecules in structures **I**–**IV** do not differ from similar values found in the Fe(II) complexes with pyridine derivatives [43, 44].

In compounds **I**–**IV**, the formation of the crystal architecture depends only on weak interactions C–H···O and C–H···π. The structure of compound **I** is a framework formed only by weak C–H···O interactions. The two-dimensional network perpendicular to the *x* axis of crystal **I** is shown in Fig. 5. Structure **II** contains chains along the *y* axis, which form channels in crystal packing. The channels include randomly arranged solvation pyridine molecules (Fig. 6) bound to the complexes through the weak C–H···π interaction. In structure **III**, the molecular iron(II) complexes form two-dimensional networks with chains of the DMF solvate molecules between them. The DMF molecules interact with the complexes to form the intramolecular hydrogen bonds C–H···O (Fig. 7). In structure **IV**, as well as in **II**, chains along the *y* axis can be distinguished, while each cavity formed by the complexes contains two MEK molecules linked by intramolecular hydrogen bonds C–H···O (Fig. 8). Other intermolecular contacts in structures **III** and **IV** correspond to the sums of the van der Waals radii of the corresponding atoms.

Thus, in crystals **I**–**IV**, the $[Fe(DfgH)_2Py_2]$ complexes form rather mobile packing of large molecules. The low energy of rotation of the phenyl radicals about the C–C bonds and the Py molecules about the Fe–N bonds allows the aromatic rings to be arranged in such a way that the crystals would accept the solvate molecules without considerable changes in their density

(Table 1). The dihedral angles between the planes of the phenyl rings and metallocycles in compounds **I**, **II**, **III**, and **IV** are 50.7° and 46.1°, 50.0° and 115.7°, 64.7° and 118.1°, and 66.6° and 113.4°, respectively. The dihedral angles between the planes of two phenyl substituents vary within 52.8°–106.8°. The turns of the aromatic rings in crystals **II**–**IV** are defined by the intermolecular interactions with the solvate molecules. Although the complexes and solvate molecules of compounds **II**–**IV** contain no classical donor groups, all changes occur against the background of the formation of weak interactions C–H···O and C–H···π.

REFERENCES

1. L. A. Chugaev, *Metallic Compounds of α-Dioximes, Collected Works* (Akad. Nauk SSSR, Moscow, 1954) [in Russian].
2. L. E. Godycki and R. E. Rundle, Acta Crystallogr. **6** (6), 487 (1953).
3. E. O. Schlemper and R. K. Murmann, Inorg. Chem. **22** (7), 1077 (1983).
4. M. Konno, A. Kashima, and I. Shirotani, Z. Kristallogr. **212** (11), 815 (1997).
5. G. Ferraris and D. Viterbo, Acta Crystallogr. **25B** (10), 2066 (1969).
6. M. S. Hussain, B. E. Salinas, and E. O. Schlemper, Acta Crystallogr., Sect. B: Struct. Sci. **35** (1979).
7. H. Endres, H. Van de Sand, and V. Dong, Z. Naturforsch., B: Chem. Sci. **33**, 843 (1978).
8. M. S. Hussain, S. A. A. Al-Hamoud, M. Z. El-Faer, and A. Khan, J. Coord. Chem. **14** (2), 91 (1985).
9. O. Bekaroglu, S. Sarisaban, A. R. Koray, and M. L. Ziegler, Z. Naturforsch., B: Chem. Sci. **32**, 387 (1977).
10. E. Frasson, R. Bardi, and S. Bezzi, Acta Crystallogr. **12** (3), 201 (1959).
11. M. M. Bishop, A. H. W. Lee, L. F. Lindoy, et al., Supramol. Chem. **17** (1–2), 37 (2005).
12. Yu. A. Simonov, P. N. Bourosh, O. A. Bologa, et al., Zh. Strukt. Khim. **40** (1), 85 (1999).
13. Yu. A. Simonov, V. Kh. Kravtsov, N. V. Gerbeleu, et al., Zh. Neorg. Khim. **44** (9), 1468 (1999) [Russ. J. Inorg. Chem. **44** (9), 1390 (1999)].
14. S. T. Malinovskii, O. A. Bologa, E. B. Korobchanu, et al., Koord. Khim. **30** (5), 363 (2004) [Russ. J. Coord. Chem. **30** (5), 339 (2004)].
15. S. T. Malinovskii, E. B. Korobceanu, O. A. Bologa, et al., Zh. Strukt. Khim. **48** (3), 532 (2007).
16. S. T. Malinovskii, E. B. Korobceanu, O. A. Bologa, et al., Zh. Strukt. Khim. **48** (4), 740 (2007).
17. S. T. Malinovskii, E. B. Korobchanu, P. N. Bourosh, et al., Koord. Khim. **34** (6), 430 (2008) [Russ. J. Coord. Chem. **34** (6), 422 (2008)].
18. C. K. Prout and T. J. Wiseman, J. Chem. Soc. A, No. 1, 497 (1964).
19. K. Bowman, A. P. Ganghan, and Z. Dori, J. Am. Chem. Soc. **94** (3), 727 (1972).
20. Yu. A. Simonov, A. A. Dvorkin, I. I. Bulgak, et al., Koord. Khim. **5** (12), 1883 (1979).
21. Yu. A. Simonov, V. E. Zubareva, I. I. Bulgak, et al., Dokl. Akad. Nauk SSSR **287** (1), 122 (1986).
22. A. A. Dvorkin, Yu. A. Simonov, T. I. Malinovskii, et al., Dokl. Akad. Nauk SSSR **234** (6), 1372 (1977).
23. D. G. Batyr and I. I. Bulgak, Izv. Akad. Nauk MoldSSR, Ser. Biol. Khim., No. 1, 77 (1971).
24. D. G. Batyr and I. I. Bulgak, Izv. Akad. Nauk MoldSSR, Ser. Biol. Khim., No. 3, 71 (1971).
25. Yu. A. Simonov, M. M. Botoshanskii, T. I. Malinovskii, et al., Dokl. Akad. Nauk SSSR **246** (3), 609 (1979).
26. L. D. Ozol, M. M. Botoshanskii, I. I. Bulgak, et al., Zh. Neorg. Khim. **25** (4), 1137 (1980).
27. Yu. A. Simonov, M. M. Botoshanskii, L. D. Ozol, et al., Koord. Khim. **7** (4), 612 (1981).
28. Yu. A. Simonov, A. A. Dvorkin, T. I. Malinovskii, et al., Koord. Khim. **11** (11), 1554 (1985).
29. Yu. A. Simonov, A. A. Dvorkin, D. G. Batyr, et al., Izv. Akad. Nauk MoldSSR, Ser. Biol. Khim., No. 3, 53 (1982).
30. Yu. A. Simonov, A. A. Dvorkin, T. I. Malinovskii, et al., Dokl. Akad. Nauk SSSR **263** (5), 1135 (1982).
31. D. G. Batyr and I. I. Bulgak, Zh. Neorg. Khim. **17** (4), 1022 (1972).
32. D. G. Batyr and I. I. Bulgak, Zh. Neorg. Khim. **17** (12), 3364 (1972).
33. D. G. Batyr and I. I. Bulgak, Zh. Neorg. Khim. **19** (8), 2205 (1974).
34. I. I. Bulgak, K. I. Turte, D. G. Batyr, and V. E. Zubareva, Koord. Khim. **10** (10), 1375 (1984).
35. XAREA, Stoe and Cie, Darmstadt, Germany, 2001.
36. R. Hooft, Collect. Nonius, Delft, Netherlands, 1980.
37. Z. Otwinowski and W. Minor, *Processing of X-Ray Diffraction Data Collected in Oscillation Mode, in Methods in Enzymology. Macromolecular Crystallography. Pt. A*, Ed. by C. W. Carter and R. M. Sweet (Academic Press, New York, 1997), vol. 276, p. 307.
38. XEMP, ver. 4.2, Siemens Analytical X-ray Inst., Inc., 1990.
39. G. M. Sheldrick, SHELX97, Program for the Refinement of Crystal Structures, Univ. of Göttingen, Germany, 1997.
40. F. H. Allen, Acta Crystallogr., Sect. B: Struct. Sci. **58** (3–4), 380 (2002).
41. I. I. Bulkhak, P. N. Bourosh, D. I. Shollmeier, et al., Koord. Khim. **35** (5), 358 (2009).
42. F. Kubel and J. Strahle, Z. Naturforsch., B: Chem. Sci. **38** (2), 258 (1983).
43. I. I. Bulgak, V. E. Zubareva, K. I. Turte, et al., Koord. Khim. **13** (7), 960 (1987).
44. S. Cakir, E. Bicer, K. Aoki, and E. Coskun, Cryst. Res. Technol. **41** (3), 314 (2006).